LOW FREQUENCY FLICKERING OF TT ARIETIS:HARD AND SOFT X-RAY EMISSION REGION

ALTAN BAYKAL and ÜMIT KIZILOĞLU
Physics Department, Middle East Technical University, Ankara 06531, Turkey

Abstract. Using archival ASCA observations of TT Arietis, X-ray energy spectra and power spectra of the intensity time series are presented for the first time. The energy spectra are well-fitted by a two continuum plasma emission model with temperatures $\sim$ 1 keV and $\sim$ 10 keV. A coherent feature at $\sim$ 0.643 mHz appeared in the power spectra during the observation.

Key words: *Subject headings:*

binaries: close -stars: individual (TT Arietis) -stars: cataclysmic variables -X-rays: stars

1. Introduction

TT Arietis has been categorized as a nova-like variable from photometric observations (Smak & Stepien 1969, Cowley et al., 1975). The system's spectroscopic orbital period is found to be 0.13755114(13)^d (Thorstensen et al., 1985) from measurements of the radial velocities of emission lines. This is longer than the photometric period of 0.1329^d (Tremko 1992). The beat frequency of the photometric and spectroscopic orbital periods is $\sim$ 0.25 d^{-1} which is very similar to the intermediate polar TV Col (Hellier et al. 1991). This led Jameson et al. (1982) to the suggestion that TT Ari is an intermediate polar. The optical brightness of TT Ari varies irregularly on long time scales. It can remain at visual magnitudes $\sim$ 10 (high state) for many years, interrupted irregularly by low states with visual magnitudes $\sim$ 16 which last less than a year (Shafter et al. 1985). In the high state, TT Ari has shown flickering activity (or quasi-periodic oscillations) with periods between 14 min and 27 min (Semeniuk et al., 1987; Hollander & van Paradijs 1992).

TT Ari was found to be a hard X-ray source by the Einstein satellite (Cordova et al., 1981). Jensen et al. (1983) investigated the correlation of X-ray and optical flickering activity using simultaneous observations with the Einstein X-ray observatory and the Mount Wilson Optical Telescope. They found that the flickering activity of X-rays at $\sim$ 17 min ($\sim$ 1 mHz) is delayed by $\sim$ 1 min with respect to the optical flickering activity. They proposed that the optical flickering in TT Ari is produced in the inner accretion disk, and a fraction of the energy is transported to a different region where the X-ray flickering is produced. The 1 min time delay between the optical and X-ray flickering would be the time required to transport energy from the optical flickering region to the X-ray emitting region (Jensen et al., 1983).

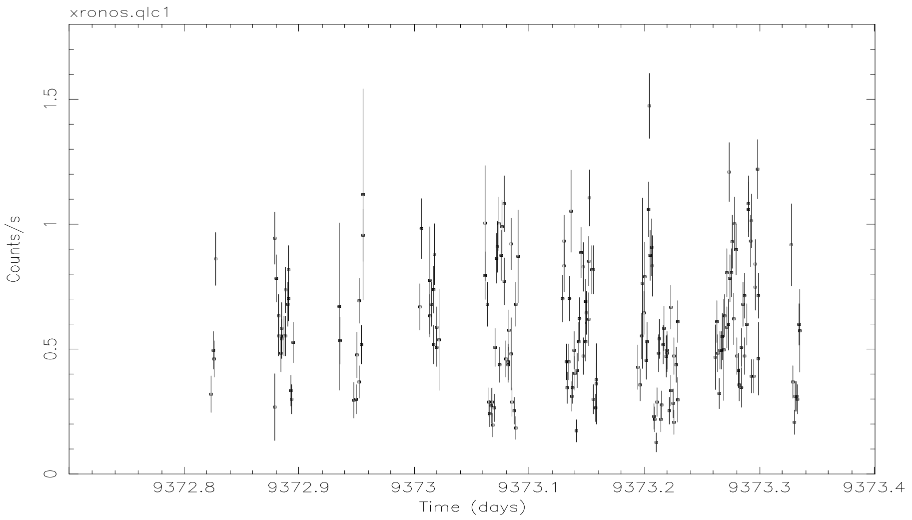

Figure 1. The light curve of TT Ari with SIS0 count rates binned in intervals of 86 sec. The times indicates MJD 40000+.

In the present work, we analyze archival ASCA data to construct the X-ray egergy spectra and power spectra of TT Ari. Section 2 describes the observations. Section 3 describes the X-ray spectra and X-ray timing.

2. Observations

TT Ari was observed with ASCA on January 20 to 21, 1994 with an effective exposure time $\sim$ 14 ksec. The ASCA instrumentation (Tanaka et al. 1994) consists of four imaging telescopes, each with a dedicated spectrometer. There are two solid-state imaging spectrometers (SIS), each consisting of 4 CCD chips, giving an energy resolution of 60-120 eV across the 0.4-10 keV band. The SIS with 2-CCD mode and GIS data were taken with a time resolution 8 sec and 62.5 msec respectively. Two gas scintillation proportional counter imaging spectrometers, GIS, have an energy resolution of 200-600 eV over the 0.8-10 keV band. Data were extracted within a $\sim$ 4 arcmin radius region for each SIS and within a $\sim$ 6 arcmin region for each GIS. The typical mean count rates of TT Ari, for the SIS and GIS are $\sim$ 0.59 and $\sim$ 0.48 count sec^{-1}, respectively. Standard cleaning for ASCA data was applied to eliminate X-ray contamination from the bright Earth, effects due to high particle background, and hot flickering SIS pixels. The reduction of the ASCA archival data and the correction of the photon arrival times to the Solar System barycenter was performed using XSPEC, XRONOS, XIMAGE and XSELECT softwares. In Fig. 1, we present the light curve of the observation.

3. Results

3.1. X-Ray Spectra

The large number of counts obtained from ASCA observations and the broad energy range (0.5-10 keV) allows for fits using various spectral models. The spectrum was fitted with a two component Raymond Smith (1977) emission model as expected from radiatively cooling shock regions. The measured unabsorbed flux during the observation was $\sim 9.74 \times 10^{-12}$ erg sec^{-1} cm^{-2} in the band of 0.5-10 keV.

In order to see the lower energy part of the spectrum (< 2 keV) more clearly and to estimate the column density N_H more accurately, ROSAT archival observations of TT Ari were extracted and a two component Raymond-Smith model was fitted to combined ASCA and ROSAT data. Our preliminary analysis showed that both data sets have similar spectra. In these fits, we assume that the spectral parameters of ASCA and ROSAT observations were the same up to a normalization factor. Results of the fit, shown in Table 1, imply that the ASCA flux was 1.1 ± 0.02 of the ROSAT flux. The column density of $N_H \sim (4.13 \pm 0.11) \times 10^{20}$ cm^{-2} obtained from the joint fit of the ROSAT and ASCA data sets is consistent with the previously deduced value from the ROSAT observation alone (Baykal et al., 1995). The two component Raymond Smith model fits the data well with $\chi^2_\nu \sim 1.03$, giving the plasma temperatures of about ~ 1 keV and ~ 10 keV, for the two components.

Keeping in mind that the spectral characteristics may change in time and while the column density probably remains constant; the column density deduced from the joint ROSAT-PSPC and ASCA-SIS0+GIS2 data was used for further spectral work with the ASCA observations. In Fig. 2, we present the energy spectra fits with the two component model. Only SIS0+GIS2 data are used for clarity.

Table 1 gives the spectral parameters for the best fit to the SIS0+GIS2 data to compare with the joint fit and two component Raymond Smith model to SIS0+SIS1+GIS2+GIS3 detectors.

Spectral results from a two temperature Mewe-Kaastra model are also given. This model gives slightly lower plasma temperatures, but it does not improve the goodness of fit.

The residuals do not indicate an extra line feature at 6.67 ± 0.03 keV. Inset in Fig. 2 shows data and the model fitted to it. To check whether a line feature component is evident for 6.43 keV which may indicate the presence of of emission from the white dwarf surface, a variable Raymond Smith model with zero Fe abundance and a Gaussian line feature is tested. The data is again well fitted with a Gaussian line at 6.67 ± 0.03 keV of a one sigma width 68 ± 39 eV and a line flux $(2.42 \pm 0.10) \times 10^{-5}$ photons cm^{-2}sec^{-1}.

In order to see the spectral modulation over the orbit, hardness ratios (2-10/0.2-2 keV) are plotted in Fig. 3. The data are folded at the spectroscopic orbital period $P=0.13755114(13)^d$ with an epoch JD= 2,443,729.0175 (Thorstensen et al., 1985). As seen from the Fig. 3, there is no significant variation of the hardness ratio. The

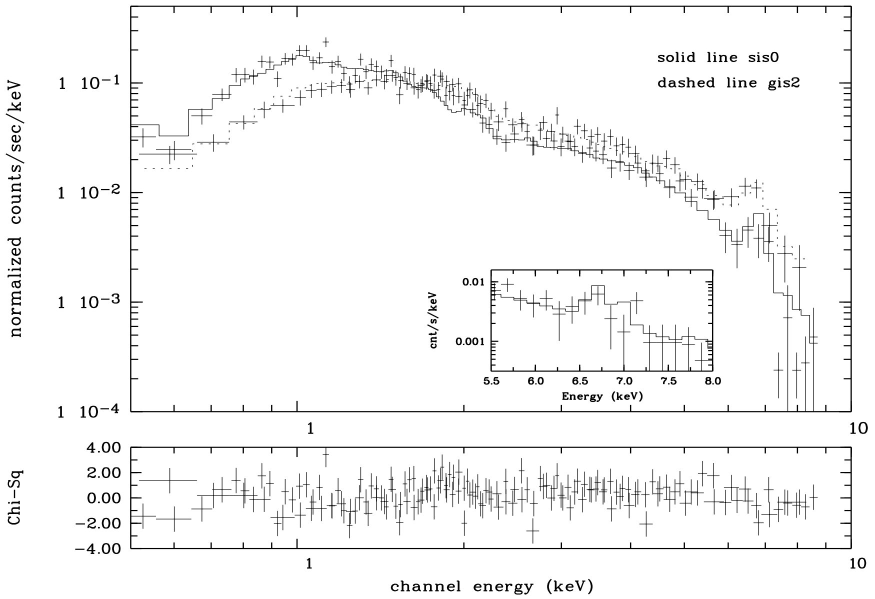

Figure 2. The average ASCA/ SIS0, GIS2 spectra of TT Ari. The upper panel shows the fit of the two component Raymond-Smith model. Data is binned for 5σ confidence. The lower panel is the χ^2 residuals from the fit. Inset shows 6.67 keV feature, binned for 3σ confidence, together with the model fitted to it.

Table I
Spectral Fit Parameters for Two Temperature Models [a]

model	kT_1(keV)	kT_2(keV)	$A_1(10^{-4})^f$	$A_2(10^{-3})^f$	$N_H(10^{20}cm^{-2})$	χ^2_ν
R-S [b]	1.03 ± 0.05	10.99 ± 1.17	4.92 ± 1.36	6.83 ± 0.14	4.13 ± 0.11	1.03
R-S [c]	0.99 ± 0.12	9.29 ± 1.02	3.70 ± 2.22	7.16 ± 0.19	4.13 fixed	0.96
R-S [d]	0.97 ± 0.08	8.49 ± 0.63	3.67 ± 1.51	7.26 ± 0.13	4.13 fixed	1.36
Meka [e]	0.76 ± 0.05	8.10 ± 0.49	3.37 ± 0.91	7.32 ± 0.09	4.13 fixed	1.48

[a] Spectral fits were performed using the program XSPEC.
[b,c,d] Raymond−Smith model for PSPC+SIS1+GIS2, SIS1+GIS2 and SIS0+SIS1+GIS2+GIS3 detectors respectively.
[e] Mewe−Kaastra model for SIS0+SIS1+GIS2+GIS3 detectors.
[f] A_1 and A_2 are the emission measures in units of $10^{-14}/(4\pi D^2)\int\ n^2dV$, where D is the distance to the source (cm) and n is the electron density (cm^{-3}).

binary orbital phases 0.75-0.9 were softer in ROSAT observations (see Baykal et al., 1995). However, as these orbital phases are occulted in the ASCA observation

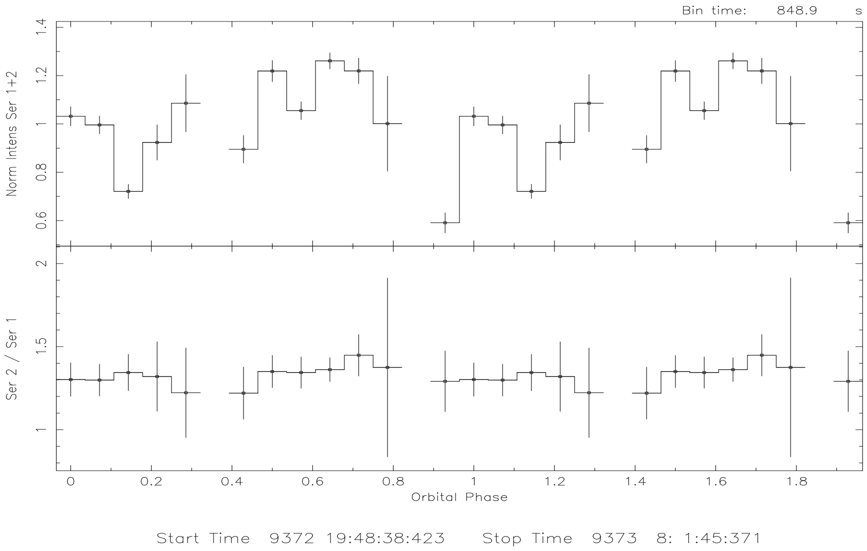

Figure 3. The upper panel is the normalized light curve folded at the spectroscopic orbital period P=0.13755114(13)^d with the epoch JD= 2443729.0175 (Thorstensen et al., 1985). The lower panel is the hardness ratio (2-10 keV/0.2-2 keV) of the light curve.

due to the satellite orbit around the earth,so we can not address this issue with the ASCA data.

3.2. X-Ray Timing

The ASCA observations were interrupted by a number of gaps. In order to examine the high frequency oscillations we calculated Fast Fourier transforms for each observation window and then averaged them.

The length of each stretch was chosen as 2048 sec with 4096 bins. The average power density spectrum is normalized according to Leahy et al. (1983) and rebinned logarithmically in frequency (see Fig. 4). In the power spectrum, the counting statistics noise (or white noise) level is around 2 since there are 2 degrees of freedom for each power estimate and each estimate obeys a χ^2 distribution (see van der Klis 1989). For frequencies higher than 10 mHz, the variability of TT Ari dissolves into the noise level which is consistent with the ROSAT observations (Baykal et al. 1995). For frequencies lower than 10 mHz, a red noise component (or flicker noise) exists.

In order to examine the flickering activity and the oscillations at lower frequencies, discrete power spectra (Deeming 1975) were estimated and normalized according to Leahy et al. (1983).

A power spectrum with 16 sec data bins is presented in Fig. 5 which has a mean value of 2 at frequencies higher than 10 mHz. A red noise component (or flicker

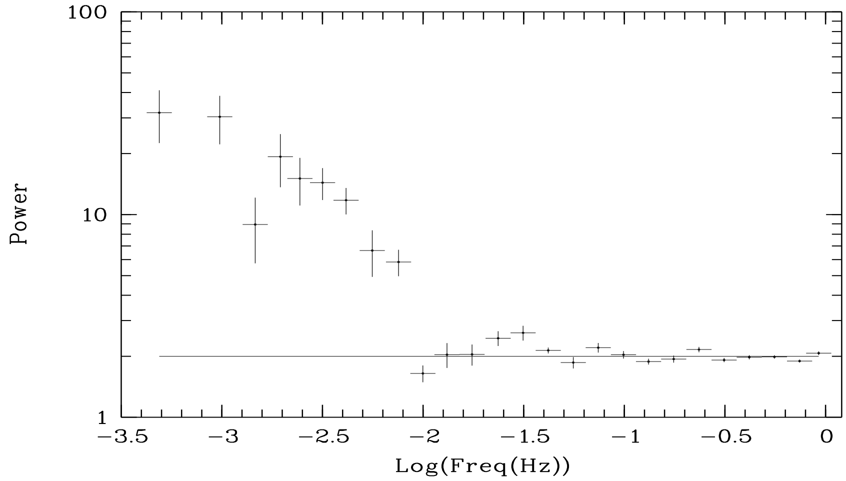

Figure 4. The average power spectrum of TT Ari. Data were binned 0.5 sec for each GIS2 and GIS3 detectors. The power spectra were averaged for each observational window and presented by log-log scale (horizontal line represents the counting statistics noise). The windows were of length 2048 seconds.

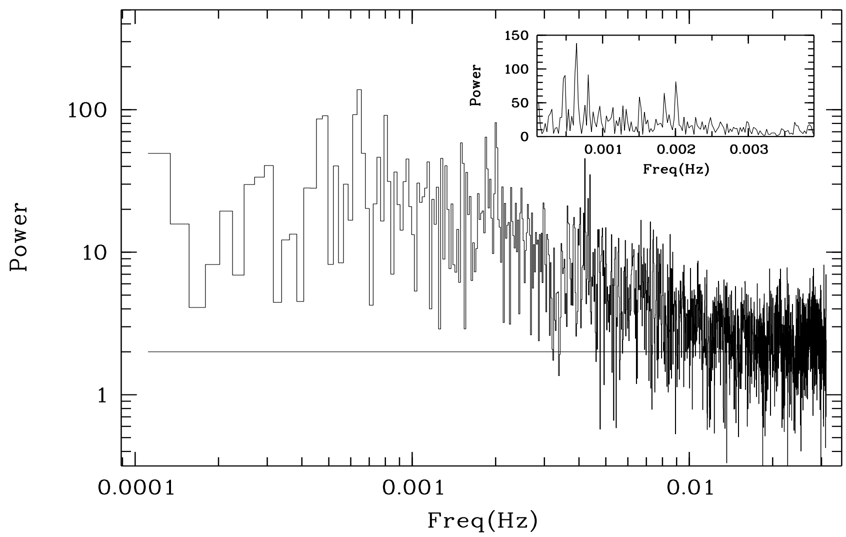

Figure 5. The average power spectrum of TT Ari for SIS0, SIS1, GIS2 and GIS3 detectors. Data were binned in 16 sec intervals for each detector. Horizontal line represents the counting statistics noise. Inset shows the lower frequency part with a linear scale.

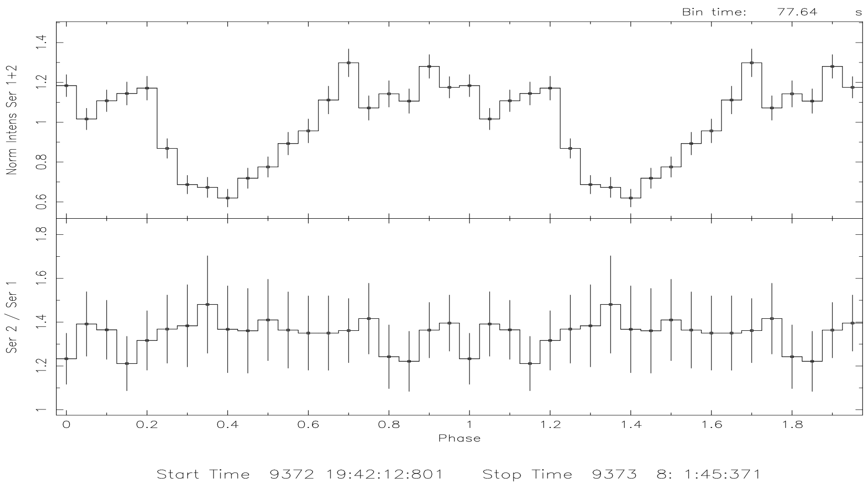

Figure 6. The upper panel is the normalized light curve folded at 1553 seconds. The lower panel is the hardness ratio (2-10 keV/0.2-2 keV) of the ligh curve.

noise) dominates at frequencies between 1mHz and 10 mHz. The noise is saturated (secondary white noise) at frequencies lower than 1mHz (see Fig. 5).

In order to search for an oscillation , we fitted a constant line to the power at frequencies lower than 1 mHz yielding the mean power <Power> = 22. In order to see the probability of detection of a significant signal above this level, an exponential probability distribution, Prob(P)=(1/2σ^2) exp (-P/2σ^2), which is essentially a χ^2 distribution for two degrees of freedom (Scargle 1982) where <Power>=2σ^2 =22, is applied. For given parameters, the confidence level of the signal for the maximum power (P_{max}=138) at 0.643 mHZ is 1-N_p exp (-P_{max}/<Power>) $\sim$ 0.9 (Leahy et al., 1983), where N_p=40 is the number of iteration frequencies between 1×10^{-4} and 1×10^{-3}. This confidence level is close to $\sim 2\sigma$ signal detection and the error in the period estimate is ΔPeriod = Period^2/ T_{obs} $\sim$ 170 sec where T is the time span of the observations. The symmetric side lobes of the peak frequency are the convolved window function of the observation gaps. These are seen at ferequencies 0.643 ± 0.17 mHz, where 0.17^{-1} mHz^{-1} $\sim$ 5582 sec is close to the orbital period of the ASCA satellite around the earth ($\sim$ 5700 sec). We also deconvolved the window function by making use of the "CLEAN" algorithm (Roberts et al., 1987) and verified the 0.643 mHz oscillation. In Fig. 6, the light curve folded at this frequency is presented together with its hardness ratio (2-10 keV/0.2-2 keV).

4. Discussion

We find that TT Ari is one of the more "sophisticated" and interesting sources among the catalysmic binaries. Our basic results are summarised below.

A soft X-ray excess around $\sim$ 1 keV has been seen In magnetic catalysmics binaries (Singh & Swank 1993, Ishida et al., 1994, Mukai et al., 1994).These systems have spin periods $10 - 10^3$ sec. According to the theories of magnetic cataclysmic binaries (such as DQ Her systems), most of the X-ray emission is received from the shock regions of the accretion columns near the white dwarf magnetic poles (Patterson 1994). The cooling plasma in the accretion column has both soft $\sim$ 1 keV and hard $\sim$ 9 keV X-ray components (Singh & Swank 1993, Ishida et al., 1994). Some spectra show the iron fluorescence line at 6.43 keV which is an indicator of emission from the white dwarf surface (Ishida et al., 1994). Although the X-ray spectra of TT Ari shows both soft and hard X-ray components, it deviates from the category of magnetic cataclysmic binaries for at least two reasons; i) the spin period of the source is not observed, ii) it does not show a 6.43 keV emission line.

EINSTEIN and ROSAT observations have shown that the upper limits of the X-ray luminosity from the late type seconderies are $L_x \sim 10^{29}$ erg/sec (Fleming et al., 1989, Hempelmann et al., 1995). This is much less than the X-ray luminosity of TT Ari ($L_x \sim 1.8 \times 10^{31}$ erg/sec for a distance of 125 pc). This rules out the possible explanation that the X-ray flux comes from the corona of the secondary star.

According to Jensen et al., (1983) the X-ray flickering lags the optical flickering by $\sim$ 1 minute. This condition implies the possibility of X-ray emission regions above and below the accretion disk. Indeed, the 6.67 keV emission line suggests the possibility of emission from an accretion disk corona as observed from several X-Ray binaries (Kallman & White 1989).

The observed quasi-periodic oscillations in the optical band show correlation with mass accretion rates (Hollander & Paradijs 1993) which can be explained by a beat frequency model, as used to explain QPOs in Low Mass X-Ray Binaries (Alpar & Shaham 1985). However, this correlation was not seen in the X-ray band. The X-ray flux is 10% higher in the ASCA observations compared to the ROSAT observations while the peak frequency of flickering oscillations (or quasi-periodic oscillation) decrease by 36% (see also Baykal et al., 1995). This is an another indicator that the X-ray flux is not directly correlated with the mass accretion rate. Furthermore, hardness ratios of the folded lightcurve (see Fig. 6) do not show absorption (or hard X-ray excess) at the dips of the lightcurve, which implies that the flickering in X-rays is not associated with occultation of blobs. Our main conclusion is that the X-ray emission may be associated with an accreation disk corona rather then directly with the accreation column. In order to improve our understanding of the flickering oscillations, multiwavelength simultaneous observations of TT Ari are required.

5. Acknowledgements

We thank the referee Prof. Dr. J.E. Dyson, for a careful reading and valuable comments. A.B acknowledges the National Research Council for their support. We also thank the *ASCA* GOF team for the archival data. This work is supported by The Scientific and Technical Research Council of Turkey, TÜBİTAK, under High Energy Astrophysics Unit.

References

Alpar M.A, Shaham J., 1985, *Nature,* **316,** 239
Baykal A., Esendemir A., Kızıloğlu Ü., et al., 1995, *Astron. Astrophys.,* **299,** 421
Cordova F.A., Mason K.O., Nelson J.E., 1981, *Astrophys. J.,* **245,** 609
Cowley A.P., Crampton, D., Hutchings, J.B., Marlborough, J.M., 1975, *Astrophys. J.,* **195,** 413
Deeming T.J., 1975, *Astron. Space Science*, **36,** 137
Fleming T.A., Giampapa M.S., Schmitt J.H.M.M., Bookbinder J.A., 1993, *Astrophys.J.,* **410,** 387
Hempelmannm A., Schmitt J.H.M.M., Schultz., et al., 1995, *Astron. Astrophys.,* **294,** 515
Hollander A., van Paradijs J., 1992, *Astron. Astrophys.,* **265,** 77
Hellier, C., Mason, K.O., Mittaz, J.P.D., 1991, *MNRAS,* **248,** 5p
Ishida M., Mukai K., Osborne J.P., 1994, *PASJ,* **46,** L81
Leahy D.A., Darbo W., Elsner R.F., et al., 1983, *Astrophys. J.,* **266,** 16
Mukai K., Ishida M., Osborne J.P., 1994, *PASJ,* **46,** L87
Kallman T., White N.E., 1989, *Astrophys. J.,* **341,** 955
Jameson R.F., King A.R., Sherrington M.R., 1982, *MNRAS,* **200,** 455
Jensen K.A., Cordova F.A., Middleditch J., et al., 1983, *Astrophys. J.,* **270,** 211
Patterson J., 1994, *PASP*, **106,** 209
Roberts D.H., Lehar J., Dreher J.W., 1987, *Astron. J.,* **93,** 968
Raymond, J., Smith, B.H., 1977, *ApJS*, **35,** 419
Robinson C.R., Cordova F.A., 1993, ASP conference proceedings entitled Intreacting Binaries (ed. A.W. Shafter)
Scargle, J.D., 1982. *Astrophys. J.,* **263,** 835
Semeniuk, I., Schwarzenberg-Czerny, A., Duerbeck,H., et al., 1987, *Acta Astron.,* **37,** 197
Shafter, A.W., Szkody, P., Liebert, J., et al., 1985, *Astrophys. J.,* **290,** 707
Smak J., Stepien K., 1969, Non-Periodic Phenomena in Variable Stars, p. 355, ed. Detre, L. (Academy Press, Budapest)
Singh J., Swank J., 1993, *MNRAS,* **262,** 1000
Tanaka Y., et al., 1994, *PASJ. Letters,* **46,** L37
Thorstensen J.R., Smak J., Hessman F.V., 1985, PASP 97, 437
Tremko, J., 1992, Inf. Bull. Var. Stars 3763
van der Klis, M., 1989, Timing Neutron Stars, ed. H.Ögelman and J. van den Heuvel, NATO/ASI, vol 262, p 27